American Mineralogist, Volume 78, pages 1–7, 1993

Mössbauer absorber thicknesses for accurate site populations in Fe-bearing minerals

D. G. Rancourt
Ottawa-Carleton Geoscience Centre and Ottawa-Carleton Institute for Physics, Department of Physics, University of Ottawa, Ottawa K1N 6N5, Canada

A. M. McDonald
Ottawa-Carleton Geoscience Centre, Department of Earth Sciences, Carleton University, Ottawa K1S 5B6, Canada

A. E. Lalonde
Ottawa-Carleton Geoscience Centre, Department of Geology, University of Ottawa, Ottawa K1N 6N5, Canada

J. Y. Ping*
Ottawa-Carleton Institute for Physics, Department of Physics, University of Ottawa, Ottawa K1N 6N5, Canada

Abstract

We define the ideal absorber thickness, t_{ideal}, in the usual way, as the absorber thickness that gives the largest signal to noise ratio in a given time, and show by measurements that it is reliably calculated in real situations by the formulae of Long et al. (1983). We identify problem areas where it is essential to use the correct t_{ideal}.

We describe thickness effects (i.e., unavoidable spectral distortions arising from nonzero absorber thicknesses) for uniform and nonpolarizing absorbers and define the thin absorber thickness, t_{thin}, as the largest thickness for which thickness effects are negligible. We present a graphical method whereby t_{thin} can be evaluated for real mineral absorbers having spectra composed of intrinsically broad lines.

The limits of our methods are carefully outlined. The necessary background concerning thickness effects in multisite materials has not been developed in the literature and is therefore given in detail.

Most often $t_{thin} \ll t_{ideal}$, however, with Fe-poor end-members (or with minerals containing Fe as a trace) one can have $t_{thin} \geq t_{ideal}$ at t_{ideal} values corresponding to quite doable experiments. We recommend that, whenever accurate quantitative results are required, the first concern be to obtain the best possible measured spectrum by using $t = t_{ideal}$. One can then reliably obtain the intrinsic absorber cross section (thereby eliminating all thickness effects) by deconvoluting the measured data using methods such as those recently developed by Rancourt (1989).

Introduction

In choosing a Mössbauer absorber thickness, n_a (in number of Mössbauer nuclei per centimeters squared), one must distinguish two characteristic thicknesses: a thin absorber thickness, $n_{a,thin}$, defined to be just small enough to reduce thickness effects (i.e., spectral distortions arising from nonzero absorber thickness and leading to incorrect spectral areas, heights, widths, and detailed shapes) to some tolerable amount (e.g., less than the error in the raw spectral area determinations) and an ideal absorber thickness, $n_{a,ideal}$, defined to give the largest signal to noise ratio (S/N) in a given time. These two characteristic thicknesses are highly sample dependent and, for a given sample, are generally significantly different.

It is common practice to use an absorber thickness that is an uncomfortable compromise between $n_{a,thin}$ and $n_{a,ideal}$ (Hawthorne, 1989). A rule of thumb that is often invoked is to use 5–10 mg/cm^2 of natural Fe. No effort is then made to estimate the degree of thickness effects at this chosen thickness. This rule of thumb originates partly from Greenwood and Gibb's (1971) correct calculation that for metallic Fe the true ideal absorber thickness corresponds to ~10 mg/cm^2 of α-Fe absorber and partly from Hawthorne's (1989) suggestion that for Fe-bearing oxide and oxysalt minerals, a good compromise between $n_{a,thin}$ and $n_{a,ideal}$ is 5 mg/cm^2 of Fe. The accurate $n_{a,ideal}$ value for a metallic Fe absorber is 16 mg/cm^2 Fe.

* Present address: University of Science and Technology Beijing, 100083 Beijing, P.R. China.

0003–004X/93/0102–0001$02.00

TABLE 1. Calculated and measured ideal Mössbauer absorber thicknesses for three representative micas in the phlogopite-annite series

Sample	Density† (g/cm³)	Wt% Fe‡	Calculated thicknesses*					Measured**
			t μm	t_g mg/cm²/mica	t_{Fe} mg/cm²/Fe	n_a§ ^{57}Fe/cm²	t_a‖	t μm
Annite M42126	3.31	29.5	156	51.6	15.2	3.51×10^{18}	6.3	160 (+40, −20)
Biotite MOC2661	3.06	14.1	230	70.4	9.93	2.29×10^{18}	4.1	230 (+40, −20)
Phlogopite (Headly)	2.86	2.85	391	112	3.19	0.736×10^{18}	1.3	370 (+50, −20)

* Calculated by the $1/\mu_e$ formula of Long et al. (1983).
** Errors given are maximum errors.
† Calculated from chemical composition and refined cell parameters. These values are within ~1–2% of the measured densities determined on a 25-mg Berman balance at room temperature using suspensions in both air and toluene.
‡ Obtained by microprobe analysis.
§ Assumes a natural abundance of ^{57}Fe/Fe of 2.14%.
‖ Dimensionless Mössbauer thickness parameter defined as $t_a \equiv f_a n_a \sigma_0$, where we assume a typical room-temperature recoilless fraction, $f_a = 0.7$, and use the value $\sigma_0 = 2.56 \times 10^{-18}$ cm² for the Mössbauer cross section at resonance.

One study (Dyar, 1984) has attempted to consider the absorber thickness problem and concludes that an optimum thickness is an Fe concentration of 5–7 mg/cm² of natural Fe that is independent of both the chemical composition of the absorber and the intrinsic spectral shape (single line vs. quadrupole doublet, etc.). Fundamental problems with the analysis leading to this optimum concentration (Dyar, 1984) have been pointed out by Waychunas (see Waychunas, 1986, 1989; Dyar, 1986, 1989).

In this paper we compare calculated and measured ideal absorber thicknesses for three micas representing the annite-phlogopite series (Table 1). The approximate calculation described by Long et al. (1983) is found to give excellent agreement with measured $n_{a,ideal}$ values. This implies that their approximation is valid for calculating accurate $n_{a,ideal}$ values in many applications (even when $n_{a,thin} \ll n_{a,ideal}$, as with the micas), and establishes their simple formula as a particularly useful tool. We, therefore, use this formula to calculate the ideal ^{57}Fe Mössbauer spectroscopy (MS) absorber thicknesses for representative classes of Fe-bearing minerals (Figs. 1, 2).

We also produce a graph (Fig. 3) that, for the first time, enables one to estimate both $n_{a,thin}$ and the degree to which different spectral areas are attenuated by thickness effects when $n_a > 0$ in real situations with intrinsically broad lines. Such broad lines are pervasive in the spectra of minerals, where they arise from hyperfine parameter distributions and dynamic effects (Rancourt, 1988, 1989; Rancourt and Ping, 1991).

THICKNESS EFFECTS AND THE THIN ABSORBER THICKNESS

In MS, the quantity that contains the desired (chemical, crystallographic, magnetic, morphological, dynamical, etc.) information is the total absorber resonant cross section:

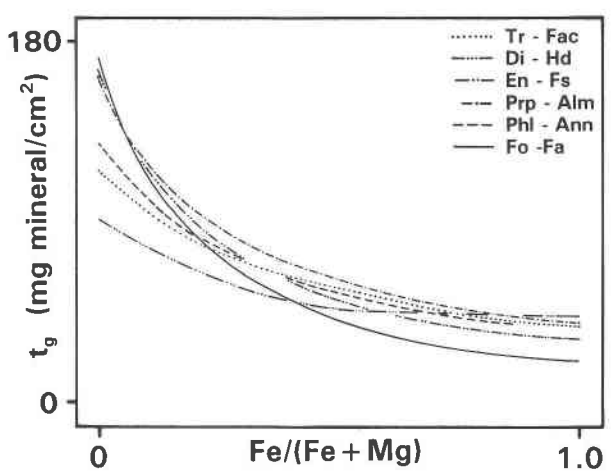

Fig. 1. Calculated ideal ^{57}Fe Mössbauer absorber thicknesses, t_g (in milligrams of mineral per centimeters squared of absorber surface), for six classes of Fe-Mg solid solutions. The calculations were performed by the $1/\mu_e$ equation of Long et al. (1983), given as Eq. 17 in this paper.

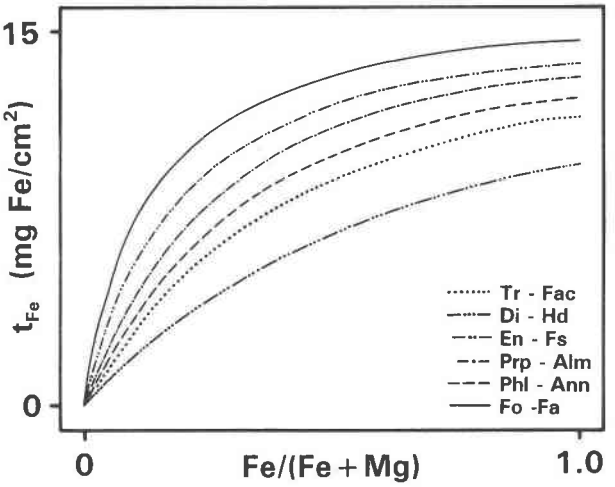

Fig. 2. Calculated ideal ^{57}Fe Mössbauer absorber thicknesses t_{Fe} (in milligrams of natural Fe in the sample per centimeters squared of absorber surface) for the same six classes of Fe-Mg solid solutions as in Fig. 1. The calculations were performed in the same way as in Fig. 1.

$$\sigma'_a(E) \equiv \sum_i \sigma'_{a,i}(E) \equiv \sum_i f_{a,i} n_{a,i} \sigma_{a,i}(E) \qquad (1)$$

where "i" is an index that runs over the different Fe sites (and ion types) in the absorber and $f_{a,i}$, $n_{a,i}$, and $\sigma_{a,i}(E)$ are site-specific absorber recoilless fractions (f factors), $^{57}Fe/cm^2$ thicknesses, and intrinsic absorber resonant cross sections, respectively. The latter intrinsic cross sections are, by definition, normalized as

$$\int_{-\infty}^{+\infty} dE\ \sigma_{a,i}(E) = \pi/2 \sigma_0 \Gamma_0 \qquad \forall i \qquad (2)$$

where Γ_0 is the natural full width at half maximum (FWHM) of the Mössbauer transition, σ_0 is the cross section at resonance for the Mössbauer transition, and $\forall i$ refers to all i. It follows that

$$\int_{-\infty}^{+\infty} dE\ \sigma'_{a,i}(E) = \pi/2 \sigma_0 \Gamma_0 f_{a,i} n_{a,i} \qquad \forall i \qquad (3)$$

and

$$\int_{-\infty}^{+\infty} dE\ \sigma'_a(E) = \pi/2 \sigma_0 \Gamma_0 \sum_i (f_{a,i} n_{a,i}). \qquad (4)$$

One goal in applying MS is to obtain $\sigma'_a(E)$, to resolve it into its site-specific components, $\sigma'_{a,i}(E)$, and, knowing the $f_{a,i}$, to obtain the site populations, $n_{a,i}$, from the areas (Eq. 3).

The total absorber resonant cross section $\sigma'_a(E)$ is, however, never observed directly. In absorption experiments, it gives rise to the measured absorption spectrum, $N(E)$. For uniform and nonpolarizing absorbers, $N(E)$ is given by the well-known transmission integral:

$$N(E) = BG + \eta_M f_s \frac{2}{\pi\Gamma_0} \int_{-\infty}^{+\infty} d\psi \frac{\Gamma_0^2/4}{(\psi + E)^2 + \Gamma_0^2/4} \cdot (e^{-\sigma'_a \psi} - 1) \qquad (5)$$

where BG is the measured background level, η_M is the part of the BG that is from both recoilless and nonrecoilless Mössbauer γ-rays, and f_s is the recoilless fraction of the single-line thin source. An absorber is uniform if all variations (on a scale of the Mössbauer cross section at resonance, σ_0, or larger) in n_a are small ($\delta n_a / n_a \ll 1$) everywhere on its exposed surface.

Until recently, only the case of a single site had been discussed in detail in the literature (Rancourt, 1989). In that case, the relevant cross section can be written as

$$\sigma'_a(E) = t_a \sigma_a(E)/\sigma_0 = f_a n_a \sigma_a(E) \qquad (6)$$

where

$$t_a \equiv f_a n_a \sigma_0 \qquad (7)$$

is the usual dimensionless thickness parameter. This factorization (Eq. 6) is again possible in the multisite case, if we define $\sigma_a(E)$ as

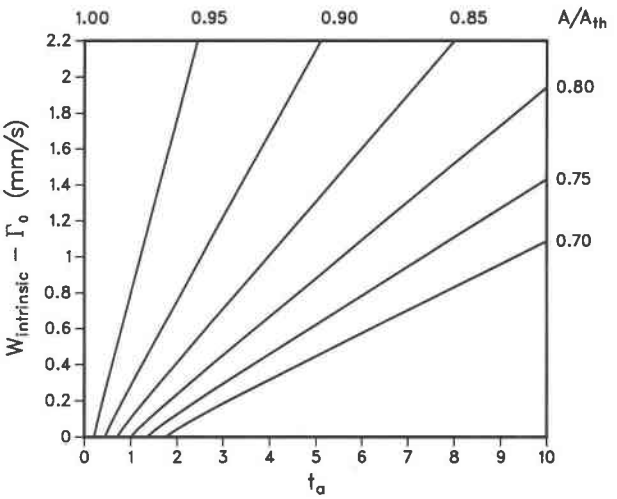

Fig. 3. Lines of equal spectral area attenuation (equal A/A_{thin}) in the plane $W_{intrinsic} - \Gamma_0$ vs. t_a. This graph allows the thin absorber thickness to be evaluated. See text for details.

$$\sigma_a(E) \equiv \frac{1}{\sum_i f_{a,i} n_{a,i}} \sum_j f_{a,j} n_{a,j} \sigma_{a,j}(E) \qquad (8)$$

such that Equations 6 and 7 are valid, where now

$$f_a \equiv \frac{1}{n_a} \sum_i n_{a,i} f_{a,i} \qquad (9)$$

and, obviously, $n_a \equiv \sum_j n_{a,j}$.

Few practitioners use the full transmission integral in analyzing their spectral data. Instead, the thin absorber condition

$$\sigma'_a(E) \equiv \sum_i \sigma'_{a,i}(E) \equiv \sum_i f_{a,i} n_{a,i} \sigma_{a,i}(E) \ll 1 \qquad \forall E \qquad (10)$$

is usually assumed. This assumption leads to the thin absorber expression for the measured spectrum

$$N_{th}(E) = BG - \eta_M f_s \frac{2}{\pi\Gamma_0} \cdot \int_{-\infty}^{+\infty} d\psi \frac{\Gamma_0^2/4}{(\psi + E)^2 + \Gamma_0^2/4} \cdot \sigma'_a \psi \qquad (11)$$

or

$$N_{th}(E) = BG - \eta_M f_s \frac{2}{\pi\Gamma_0} \sum_i f_{a,i} n_{a,i} \cdot \int_{-\infty}^{+\infty} d\psi \frac{\Gamma_0^2/4}{(\psi + E)^2 + \Gamma_0^2/4} \cdot \sigma_{a,i} \psi \qquad (12)$$

where one has performed a Taylor expansion of the exponential term in the integrand of the transmission integral.

This expression (Eq. 12) has relatively desirable properties that have motivated its overuse. These are (1) each site-specific absorption (i.e., spectral area) is equal to

$\pi\sigma_0\Gamma_0\eta_M f_s f_{a,i} n_{a,i}/2$ and is therefore directly proportional to $n_{a,i}$, (2) subspectral areas are additive, such that the total spectral area is

$$\int_{-\infty}^{+\infty} dE[BG - N_{th}(E)] = \tfrac{1}{2}\sigma_0\Gamma_0\eta_M f_s \sum_i f_{a,i} n_{a,i} \quad (13)$$

and (3) if $\sigma'_a(E)$ is a sum of Lorentzian lines (or a continuous distribution of Lorentzian lines, as in the case of the Voigt line shape) then the corresponding measured spectrum consists of the same sum (or distribution) but with each Lorentzian FWHM increased by the source line width Γ_0.

If the thin absorber condition (Eq. 10) is not sufficiently satisfied, then one cannot take advantage of the thin absorber expression (Eqs. 11, 12) or make use of any of its properties. Instead, one must either fit directly with the transmission integral or deconvolute out $\sigma'_a(E)$ from the measured data (Rancourt, 1989; Rancourt and Ping, 1991).

We may now describe how $n_{a,thin}$ can be evaluated for a particular absorber. Any such criterion is necessarily somewhat arbitrary.

Each line in the spectrum will have its depth, area, width, and detailed spectral shape affected by different amounts, depending on the extent to which the thin absorber condition (Eq. 10) is satisfied for that line. On comparing the observed line given by Eq. 5 with that predicted by the thin absorber limit (Eq. 11), one notes that the depth is affected more than the area, which is affected more than the width (see Ping and Rancourt, 1992, for explicit demonstrations of these points). Since area is often of primary concern, we define $n_{a,thin}$ with reference to the ratio (A/A_{th}) of the observed area to the thin limit line area. For any $n_a \neq 0$, $A < A_{th}$, and for a thin absorber $A/A_{th} \simeq 1$.

We choose a tolerable value of A/A_{th}, say 0.98 or 0.95 (spectral areas can often be evaluated with precisions of a few percent), that defines $n_{a,thin}$ for a given intrinsic line width, W_{int} [i.e., a true FWHM of the corresponding line in $\sigma'_a(E)$]. This is shown in Figure 3 where lines of constant A/A_{th} are drawn in the plane of $W_{int} - \Gamma_0$ vs. t_a. Figure 3 is calculated by the methods of Ping and Rancourt (1992). Since widths are affected much less than areas, the observed FWHM, W_{obs}, is related to W_{int} as

$$W_{obs} \simeq W_{int} + \Gamma_0. \quad (14)$$

This implies that if an absorber has known values of f_a (or some representative value) and n_a (known from elemental analysis) and has a fraction, α, of its spectral area in its deepest line of observed width, $W_{obs,d}$, then its approximate Figure 3 coordinates are

$$W_{int} - \Gamma_0 \simeq W_{obs,d} - 2\Gamma_0 \quad \text{and} \quad t_a \simeq \alpha f_a n_a \sigma_0 \quad (15)$$

such that one easily determines whether it is thin or thick. The crossover occurs at $n_a = n_{a,thin}$ and thus defines $n_{a,thin}$.

Figure 3 can also be used to estimate thickness corrections to spectral areas of separate lines in a given observed spectrum. It gives a quantitative estimate of how individual lines in a spectrum are affected differently. We do not recommend these uses of Figure 3 as substitutes for using either the correct transmission integral or an appropriate deconvolution. For partially overlapping lines, spectral distortions arising from finite thickness are such that fitted areas in raw spectra can be significantly wrong by more than just the expected attenuation predicted in Figure 3, because of the effects that the spectral distortions have on fitted line tradeoffs (e.g., Hargraves et al., 1989).

Ideal and thin absorber thicknesses in the phlogopite-annite series

Absorber thickness can be expressed in various ways: n_a (in $^{57}Fe/cm^2$) and t_a (dimensionless) have already been defined and are related by Equation 7; $t_a \equiv \sigma_0 \Sigma f_{a,i} n_{a,i}$ corresponds to the average number of Mössbauer nuclei encountered by a γ-ray traversing the sample at any point. Given the concentration of ^{57}Fe in the sample, these can be related to a thickness, t_{Fe}, expressed in milligrams of Fe per centimeters squared. Given the mean absorber stoichiometry, this in turn corresponds to a thickness, t_g, expressed in grams (or milligrams) of absorber material per centimeters squared. Finally, if the material density, ρ, is known, an actual physical thickness, t (in micrometers, say), can be calculated by $t = t_g/\rho$.

The ideal absorber thickness arises because too thin an absorber has too little ^{57}Fe to give an appreciable resonance absorption (i.e., signal), and too thick an absorber causes too much ordinary mass absorption of the γ-rays for significant statistics to be accumulated. It depends on the material from which the absorber is made, on the absorber resonance cross section $[\sigma'_a(E)]$, and on some of the experimental circumstances (Long et al., 1983; Sarma et al., 1980; Blamey, 1977; Shimony, 1965).

Long et al. (1983) have pointed out that, with the assumption that resonance absorption is proportional to absorber thickness, an ideal absorber thickness is calculated that is both independent of $\sigma_a(E)$ and predominantly determined by the ordinary mass absorption of the absorber. Their result is that (1) when the non-Mössbauer background is small,

$$t_{g,ideal} = 2/\mu_e, \qquad (BG - \eta_M)/BG \ll 1 \quad (16)$$

and (2) when the non-Mössbauer background is large,

$$t_{g,ideal} = 1/\mu_e, \qquad (BG - \eta_M)/BG \gg 1 \quad (17)$$

where μ_e is the electronic (i.e., ordinary, nonresonance) mass absorption coefficient of the absorber material for the Mössbauer (14.4 keV) γ-rays.

The first situation (Eq. 16) is expected when, as is common practice, a narrow counting window is set on the Mössbauer γ-rays and the μ_e is small. The other limiting case (Eq. 17) occurs when either no window is used, thereby allowing many non-Mössbauer γ-ray counts, or μ_e is large because of the presence of relatively heavy elements, or both (Long et al., 1983).

The mass absorption coefficient of an absorber is calculated using its mass fractions, β_i, of the element i, as

$$\mu_e = \sum_i \beta_i \mu_{e,i}. \quad (18)$$

For example, at 14.4 keV, $\mu_{e,Fe} = 64$ cm^2/g such that $1/\mu_e = 16$ mg/cm^2 for a metallic Fe foil. This corresponds to a 20-μm foil. Long et al. (1983) have tabulated the μ_e of the elements at the important Mössbauer transition γ-ray energies.

We have compared the approximate predictions of Long et al. (1983) (above, Eqs. 16, 17) with measured ideal thicknesses of three micas belonging to the phlogopite-annite series. These consisted of specimens of single-crystal near-end-member annite (M42126, Mont St. Hilaire, Québec), biotite (MOC2661, Silver Crater mine, Bancroft, Ontario) and near-end-member phlogopite (Headley mine, Québec), all of which have been extensively studied and well characterized (Rancourt et al., in preparation; Hargraves et al., 1989).

The S/N ratios for the two strongest mica lines at approximately -0.1 and approximately $+2.3$ mm/s (with respect to α-Fe at room temperature) were measured for absorbers of various thicknesses from the three samples. The γ-ray incidence was normal to the cleavage plane. Graphs of S/N for spectra obtained in equal times (typically several minutes to several hours) vs. wafer thickness showed distinct maxima occurring at the same ideal thicknesses for the two absorption lines of a given sample.

The resulting measured ideal thicknesses for the annite, biotite, and phlogopite are, respectively, 160 (+40, −20), 230 (+40, −20), and 370 (+50, −20) μm, where maximum errors are indicated. These are in excellent agreement with the predicted values for the case of large non-Mössbauer background (Eq. 17), as seen in Table 1.

The experiments were performed with a relatively broad counting window (i.e., single-channel analyzer window larger than the FWHM of the 14.4-keV line in the pulse-height analysis spectrum). The small non-Mössbauer background case (Eq. 16) or some intermediate case might hold for an optimized counter window or a different counter, etc. Each spectroscopist must determine which case applies to his or her particular operating conditions. We expect that in most instances, with the most common Fe-bearing minerals (next section), the large background case will apply.

The important point here is that the approximate Equations 16 and 17 give the correct bounds for ideal thicknesses in real situations. This is further supported by the fact that, for each mica studied, the two absorption lines (with significantly different intensities at normal incidence, $\alpha \simeq 0.65$) gave the same ideal thicknesses. This is true even though $n_{a,thin} \ll n_{a,ideal}$ in our samples.

Using Figure 3, the line $A/A_{th} = 0.98$ (not shown), and $W_{int} - \Gamma_0 \simeq 0.3$–$0.4$ mm/s, we estimate that in all micas $t_{a,thin} \simeq 0.2$, corresponding to $n_{a,thin} \simeq 0.2 \times 10^{18}$ ^{57}Fe/cm^2 at normal incidence. This gives thin absorber wafer thicknesses of approximately 8, 20, and 90 μm, respectively, for our annite, biotite, and phlogopite. These are clearly smaller than the ideal thicknesses.

By comparison, adopting the rule of thumb using 5–10 mg/cm^2 Fe in micas causes an area attenuation of the strongest line ($\alpha \simeq 0.65$) of ~10–20% ($A/A_{th} \simeq 0.8$–0.9) and a relative attenuation difference for the two strongest lines of ~4–16% (i.e., area ratios between the two strongest lines will be incorrect and closer to 1 by this amount—for a single crystal wafer at normal incidence).

In conclusion, our mica samples have a wide range of ideal thicknesses that are accurately given by the large non-Mössbauer background expression (Eq. 17) of Long et al. (1983). This implies that the expressions of Long et al. (Eqs. 16, 17) give the correct bounds for real situations. In addition, for all of our mica samples, $n_{a,thin} \ll n_{a,ideal}$, and using either the correct $n_{a,ideal}$ values or a rule-of-thumb value results in spectra that are significantly altered by thickness effects.

Note that single-crystal wafers such as our mica samples are not nonpolarizing absorbers. Their spectra must therefore suffer from more severe thickness effects than those predicted by both Equation 5 and Figure 3; both assume nonpolarizing absorbers. In such cases, the thin absorber thickness obtained from Figure 3, as explained above, must be viewed as an overestimate. The correct t_{thin} for polarizing absorbers (single crystals, mosaic samples, nonrandom powders, magnetized ferromagnets, etc.) is smaller than the t_{thin} predicted for nonpolarizing absorbers. Methods for thickness-correcting spectra with intrinsically broad lines from polarizing absorbers have not been developed.

Ideal absorber thicknesses of Fe-bearing minerals

Values of $t_{g,ideal}$ calculated using Equation 17 are shown vs. composition in Figure 1 for several mineral groups having Mg-Fe solid solutions. Although more material is required as the Fe content decreases, when the Fe content is very small, far less material is required than would result from applying the rule of thumb of 5–10 mg/cm^2 Fe. This is seen in Figure 2, where the ideal t_{Fe} values are shown for the same mineral groups as in Figure 1. These all go monotonically to zero as the Mg end-member is approached.

Figures 1 and 2, therefore, illustrate a major breakdown in the usual rule of thumb: it suggests thicknesses that are orders of magnitude too large when Fe contents are low. Indeed, one sees that, with such Fe-poor solid solutions, it is quite possible to have $n_{a,thin} > n_{a,ideal}$. It is also in just such cases that having the correct ideal thickness will often make the difference between the detectability of the signal and the impossibility of obtaining a spectrum. With more Fe-rich minerals, the longer times required by not optimizing absorber thicknesses will often not be prohibitive, but they can easily be with Fe-poor samples.

On the other hand, it is correct to conclude (Fig. 2)

that, when Fe/(Fe + Mg) > 0.2 in the major Fe-Mg solid solutions, the ideal thicknesses range from low values of ~2–5 mg/cm² Fe to high values [at Fe/(Fe + Mg) = 1] of ~6–15 mg/cm² Fe—not far from the rule of thumb (5–10 mg/cm² Fe). We expect, however, that in most of these cases, $n_{a,thin} \ll n_{a,ideal}$ such that thickness effects are significant at these ideal thicknesses.

As a concrete example, consider near end-member phlogopite: $KMg_{2.95}Fe_{0.05}Si_3AlO_{10}(OH)_2$. This particular mineral has $n_{a,ideal} \simeq n_{a,thin} \simeq 0.2 \times 10^{18}$ $^{57}Fe/cm^2$, where $n_{a,thin}$ is approximately the same for all micas and was calculated in the previous section. This value of $n_{a,ideal}$ for this phlogopite, corresponds to ~0.8 mg/cm² Fe or to ~120 mg/cm² of the sample. On the other hand, the rule of thumb would require 5–10 mg/cm² Fe or 750–1500 mg/cm² of the sample. This would cause an ordinary mass attenuation of the incident γ-radiation that would be ~10^2–10^4 times too large, meaning that the Mössbauer radiation getting through the sample and being counted would be only ~1–0.01% of the amount that gets through at the correct ideal thickness of 0.8 mg/cm² Fe. Although the experiment is comfortably doable with the correct $n_{a,ideal}$, it becomes impossible at 10 mg/cm² Fe.

In addition to Fe-poor minerals, another area of difficulty will correspond to less common Fe-bearing minerals containing large amounts of elements with large electronic (i.e., ordinary) mass absorption coefficients. We must anticipate problems with minerals containing large mass fractions of elements with μ_e at 14.4 keV larger than approximately 100 cm²/g. Such elements (see table given by Long et al., 1983) are, with few exceptions, those with atomic numbers larger than ~60, plus the particular absorption edge group Ga, Ge, As, Se, Br, and Kr, with relatively small atomic numbers. With such minerals, especially if they also contain only small amounts of Fe, it will again be essential to use the correct ideal thicknesses.

As a final warning, we remind readers that all the results of the present paper (calculations of both thin and ideal thicknesses) are for uniform absorbers in which the depthwise average distributions of ^{57}Fe and of all the elements are uniform on every length scale of $\sqrt{\sigma_0} \simeq 0.16$ Å or larger on the sample surface. This means that only small variations in all the depth-wise average numbers of intersections with the relevant specific cross sections can be tolerated, as steps of 0.16 Å or larger are taken on the sample's exposed surface. As the variations become comparable to the numbers themselves ($\delta N \sim N$) the results presented here become invalid. Also, polarization effects have not been considered. With textured, nonrandom, mosaic, magnetized, or single-crystal absorbers, these can be significant effects and should be included in the transmission integral: see Housley et al. (1968, 1969) for the case of a simple compound having elemental absorption lines.

Nonuniformity occurs in particular with granular absorbers consisting of large grains with comparable spaces between the grains. Here using average thicknesses can lead to calculated $n_{a,thin}$ and $n_{a,ideal}$ values that are off by an order of magnitude or more. Such granular absorbers will exhibit much more severe thickness spectral distortions than would be expected from their mean thicknesses. These difficulties can often be avoided by using uniformly spread finely powdered absorbers (small grains compared with the sample thickness in micrometers). In addition, such fine powders having random orientations do not give rise to polarization effects.

Zoning of Fe content in mineral samples and whole-rock spectra of rocks containing several phases with different Fe contents are two more obvious problem areas. With such cases, one must resort to trial and error first to find thicknesses that give acceptable spectra and then to explore changes in thickness distortions arising from different nominal thicknesses. Thickness distortions are presently virtually impossible to correct in these cases. Different spectral components from different positions in the samples can have very different degrees of both spectral distortions and observability.

Recommendations

Before choosing an ^{57}Fe Mössbauer absorber thickness for a particular material, spectroscopists should know (1) which thickness (t_{ideal}) will give the largest S/N ratio, (2) which thickness (t_{thin}) will ensure that, as long as $t \leq t_{thin}$, thickness-effect spectral distortions will not be significant, and (3) in considering a compromise between t_{ideal} and t_{thin} (when $t_{ideal} > t_{thin}$), what the thickness effects will be in the measured spectrum collected at the compromise thickness. Alternatively, if the absorber thickness cannot be imposed or if the spectroscopist does not care to optimize it, then the key question is: what are the thickness effects in this situation?

In this paper, the above points are addressed for real situations involving spectra with intrinsically broad lines. Using the figures and methods described here, spectroscopists can evaluate t_{thin} and the degree of thickness attenuation of peak areas for given thicknesses of their particular materials. They can also confidently use the expressions of Long et al. (1983) (Eqs. 16, 17) to calculate t_{ideal} for the particular absorber.

In all cases, the largest thickness one would ever use is t_{ideal}. When $t_{thin} > t_{ideal}$, one uses $t = t_{ideal}$ and one is certain of collecting the best possible spectrum (largest S/N in a given time) that also has only negligible thickness effects. When $t_{thin} < t_{ideal}$, either one uses $t = t_{thin}$, thereby sacrificing spectrum quality in order to reduce thickness effects to some predetermined tolerable level, or one uses $t = t_{ideal}$ to obtain a high-quality spectrum that contains significant thickness effects that one rigorously takes into account, either by fitting with the full transmission integral (e.g., Eq. 5 in the absence of polarization effects) or by deconvoluting out the total absorber-resonant cross section (Rancourt, 1989; Rancourt and Ping, 1991).

No compromise is needed when $t_{thin} > t_{ideal}$. In the case where $t_{thin} < t_{ideal}$, most routine work will use $t = t_{thin}$, which is a compromise of known consequence, given the tolerance level chosen by the user in using Figure 3 to

calculate t_{thin}. For accurate site populations, we recommend using $t = t_{ideal}$ and deconvolution (Rancourt, 1989; Rancourt et al., in preparation).

Acknowledgments

We thank G. Robinson of the Canadian Museum of Nature for sample MOC2661 and J.A. Mandarino of the Royal Ontario Museum for sample M42126. We thank G.A. Waychunas for critically reading a first version of the manuscript. Financial support from the Natural Sciences and Engineering Research Council of Canada in the form of operating grants to D.G.R. and A.E.L. is gratefully acknowledged.

References cited

Blamey, P.J. (1977) The area of a single line Mössbauer absorption spectrum. Nuclear Instruments and Methods, 142, 553–557.

Dyar, M.D. (1984) Precision and interlaboratory reproducibility of measurements of the Mössbauer effect in minerals. American Mineralogist, 69, 1127–1144.

——— (1986) Practical application of Mössbauer goodness-of-fit parameters for evaluation of real experimental results: A reply. American Mineralogist, 71, 1266–1267.

——— (1989) Applications of Mössbauer goodness-of-fit parameters to experimental spectra: Further discussion. American Mineralogist, 74, 688.

Greenwood, N.N., and Gibb, T.C. (1971) Mössbauer spectroscopy, 659 p. Chapman and Hall, London.

Hargraves, P., Rancourt, D.G., and Lalonde, A.E. (1989) Single-crystal Mössbauer study of phlogopite mica. Canadian Journal of Physics, 68, 128–144.

Hawthorne, F.C. (1989). Mössbauer spectroscopy. In Mineralogical Society of America Reviews in Mineralogy, 18, 255–333.

Housley, R.M., Gonser, U., and Grant, R.W. (1968) Mössbauer determination of the Debye-Waller factor in single-crystal absorbers. Physical Review Letters, 20, 1279–1282.

Housley, R.M., Grant, R.W., and Gonser, U. (1969) Coherence and polarization effects in Mössbauer absorption by single-crystals. Physical Review, 178, 514–522.

Long, G.J., Cranshaw, T.E., and Longworth, G. (1983) The ideal Mössbauer effect absorber thicknesses. Mössbauer Effect Reference Data Journal, 6, 42–49.

Ping, J.Y., and Rancourt, D.G. (1992) Thickness effects with intrinsically broad absorption lines. Hyperfine Interactions, 71, 1433–1436.

Rancourt, D.G. (1988) Pervasiveness of cluster excitations as seen in the Mössbauer spectra of magnetic materials. Hyperfine Interactions, 40, 183–194.

——— (1989) Accurate site populations from Mössbauer spectroscopy. Nuclear Instruments and Methods in Physics Research, B44, 199–210.

Rancourt, D.G., and Ping, J.Y. (1991) Voigt-based methods for arbitrary-shape static hyperfine parameter distributions in Mössbauer spectroscopy. Nuclear Instruments and Methods in Physics Research, B53, 85–97.

Sarma, P.R., Prakash, V., and Tripathi, K.C. (1980) Optimization of the absorber thickness for improving the quality of a Mössbauer spectrum. Nuclear Instruments and Methods, 178, 167–171.

Shimony, U. (1965) Condition for maximum single-line Mössbauer absorption. Nuclear Instruments and Methods, 37, 348–350.

Waychunas, G.A. (1986) Performance and use of Mössbauer goodness-of-fit parameters: Response to spectra of varying signal/noise ratio and possible misinterpretations. American Mineralogist, 71, 1261–1265.

——— (1989) Applications of Mössbauer goodness-of-fit parameters to experimental spectra: A discussion of random noise versus systematic effects. American Mineralogist, 74, 685–687.

Manuscript received February 13, 1992
Manuscript accepted August 29, 1992